

# Giant spin rotation in the normal metal/quantum spin Hall junction

Takehito Yokoyama<sup>1</sup>, Yukio Tanaka<sup>1</sup>, and Naoto Nagaosa<sup>2,3</sup>

<sup>1</sup>Department of Applied Physics, Nagoya University, Nagoya, 464-8603, Japan

<sup>2</sup>Department of Applied Physics, University of Tokyo, Tokyo 113-8656, Japan

<sup>3</sup>Cross Correlated Materials Research Group (CMRG), ASI, RIKEN, WAKO 351-0198, Japan

(Dated: October 27, 2018)

We study theoretically reflection problem in the junction between a normal metal and an insulator characterized by a parameter  $M$ , which is a usual insulator for  $M > 0$  or a quantum spin Hall system for  $M < 0$ . The spin rotation angle  $\alpha$  at the reflection is obtained in the plane of  $M$  and the incident angle  $\theta$  measured from the normal to the interface. The  $\alpha$  shows rich structures around the quantum critical point  $M = 0$  and  $\theta = 0$ , i.e.,  $\alpha$  can be as large as  $\sim \pi$  at an incident angle in the quantum spin Hall case  $M < 0$  because the helical edge modes resonantly enhance the spin rotation, which can be used to map the energy dispersion of the helical edge modes. As an experimentally relevant system, we also study spin rotation effect in quantum spin Hall/normal metal/quantum spin Hall trilayer junction.

PACS numbers: 73.43.Nq, 72.25.Dc, 85.75.-d

The ultimate goal of the spintronics is to manipulate the spins without the magnetic field, and the relativistic spin-orbit interaction is the key to realize it. One example is the Datta-Das spin transistor [1] where the spin-orbit interaction modified by the gate voltage controls the rotation of the spins of the carriers. However, usually the strength of the spin-orbit interaction is weak and its influence is small especially in semiconductors. Nevertheless, its effects are now clearly observed experimentally, e.g., in the Rashba spin splitting [2], and spin Hall effect (SHE) [3, 4, 5, 6]. Further enhancement of the spin-orbit effects in semiconductors is highly desired, and for that purpose we propose in this Letter to use the quantum spin Hall (QSH) system [7, 8] and its junction to the normal metal (N) as the spin rotator with a giant angle  $\alpha$  of the order of  $\pi$  due to the resonance with the helical edge channels. This effect can be used to map the energy dispersion of the helical edge modes, and also to produce the spin current parallel to the interface with the average over the incident angle.

Naively, QSH system can be regarded as the two copies of the integer quantum Hall systems for up and down spins with the opposite chiralities. Hence, the chiral edge modes for up and down spins with the opposite propagating directions are expected, which is called the helical edge modes [9, 10, 11, 12]. Two sets of the helical edge modes can be mixed by e.g., the impurity scattering, and open the gap, but when the number of these sets is odd, i.e.,  $Z_2 = 1$ , there always remains a helical mode pair which is protected by the Kramers theorem associated with the time-reversal symmetry. The phase transition between the trivial insulator ( $Z_2 = 0$ ), and the topological insulator ( $Z_2 = 1$ ) occurs at the gap closing point, where the mass of the Dirac Fermion changes sign [13, 14].

The existence of the QSH state has been predicted in semiconductors with an inverted electronic gap in HgTe/CdTe quantum wells [13]. The quantum well sys-

tem experiences a quantum phase transition by changing the thickness. Recent experiment has successfully demonstrated the existence of the helical edge mode for the quantum well of HgTe system by the measurement of the quantized charge conductance [15]. Also recently, one can obtain the system very close to the quantum critical point by tuning the thickness of the quantum well. [16]

Most of the previous works on QSH states have focused on properties of isolated QSH system, in particular, edge states of the system. However, in experiments to detect some characteristics of the QSH system, some probe, e.g. (metallic) electrode should be attached to the QSH. Therefore, it is an important issue to clarify transport property in N/QSH junctions. Moreover, the spin transport related to the QSH system is the most interesting issue, which has not been well explored and we will address in this paper. Especially, we focus on the spin transport properties *normal* to the edge of the sample, while most of the previous works are interested in the charge transport *along* the edge channel.

In this paper, we study a reflection of the electronic wave at the N/QSH interface. It is found that an electron injected from the normal metal shows a spin dependent reflection at the interface leading to the spin rotation. The spin rotation angle  $\alpha$  shows rich structure centered around the quantum critical point  $M = 0$ , and the normal incident angle  $\theta = 0$ , i.e., it has a large value comparable to  $\pi$  and even a winding by  $4\pi$  in the  $(\theta - M)$ -plane in the QSH region ( $M < 0$ ), which stems from the helical edge modes. This is in sharp contrast to the case of normal metal/usual insulator interface. As an experimentally relevant system, we also investigate multiple reflections in QSH/N/QSH junction. It is clarified that the multiple reflection strongly enhances the spin rotation.

Let us commence with the the effective 4-band model

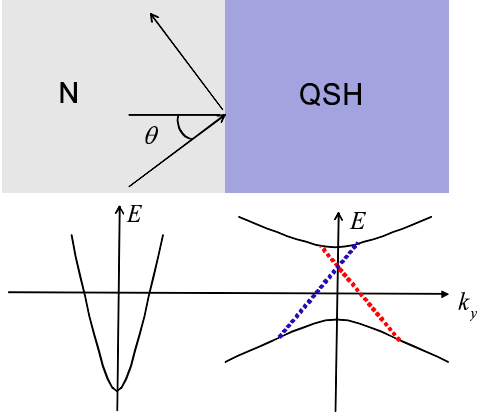


FIG. 1: (Color online) N/QSH junction and corresponding band structures (below). Dotted lines represent helical edge modes.

proposed for HgTe/CdTe quantum wells [17]

$$\mathcal{H} = \begin{pmatrix} h(k) & 0 \\ 0 & h^*(-k) \end{pmatrix}, \quad (1)$$

with  $h(k) = \epsilon(k)\mathbb{I}_{2 \times 2} + d_a(k)\sigma^a$ ,  $\epsilon(k) = C - D(k_x^2 + k_y^2)$ ,  $d_a(k) = (Ak_x, -Ak_y, M(k))$ , and  $M(k) = M - B(k_x^2 + k_y^2)$  where we have used the basis order  $(|E_1+\rangle, |H_1+\rangle, |E_1-\rangle, |H_1-\rangle)$  ("E" and "H" represent the electron and hole bands, respectively), and,

$A, B, C, D$ , and  $M$  are material parameters that depend on the quantum well geometry.  $\mathcal{H}$  is equivalent to two copies of the massive Dirac Hamiltonian but with a  $k$ -dependent mass  $M(k)$ . [17] This model is derived from the Kane model near the  $\Gamma$  point in a quantum well of HgTe/CdTe junction, and its validity is limited only near the  $\Gamma$  point, namely for small values of  $k_x$  and  $k_y$ . In this system, the transition of electronic band structure occurs from a normal to an inverted type when the thickness of the quantum well is varied through a critical thickness. This corresponds to the sign change of the mass  $M$  of this system. [13, 18]

We consider the interface between normal metal and an insulator, the latter of which is a usual insulator for  $M > 0$  and a QSH system for  $M < 0$ , as shown in Fig. 1. For  $M < 0$ , helical edge modes are expected to appear at the interface. [13, 18] The interface is parallel to  $y$ -axis and located at  $x = 0$ , and the energy dispersion of each side is shown schematically in Fig. 1. The insulating side is described by the Hamiltonian given in Eq.(1). The Hamiltonian in the N side is given by setting  $A = B = M = 0$  in that of QSH. The gap  $|M|$  opens on the insulating side.  $|C|$  is the Fermi energy measured from the bottom of the metallic band.

Now, let us focus on the spin up state, corresponding to the upper block of the Hamiltonian. Wave function in the N side for  $E_1$  state injection is given by

$$\psi(x \leq 0) = \left[ \begin{pmatrix} 1 \\ 0 \end{pmatrix} e^{ik_F \cos \theta x} + r_E \begin{pmatrix} 1 \\ 0 \end{pmatrix} e^{-ik_F \cos \theta x} + r'_E \begin{pmatrix} 0 \\ 1 \end{pmatrix} e^{-ik_F \cos \theta x} \right] e^{ik_F \sin \theta y} \quad (2)$$

with  $k_F^2 = C/D$  and the incident angle  $\theta$ .

Wave function in the QSH side reads

$$\psi(x \geq 0) = \left[ t \begin{pmatrix} Ak_+ e^{i\theta_+} \\ d(k_+) - M(k_+) \end{pmatrix} e^{ik_+ \cos \theta_+ x} + t' \begin{pmatrix} Ak_- e^{i\theta_-} \\ d(k_-) - M(k_-) \end{pmatrix} e^{ik_- \cos \theta_- x} \right] e^{ik_F \sin \theta y} \quad (3)$$

with  $d(k) = \sqrt{A^2 k^2 + M(k)^2}$  and

$$k_{\pm}^2 = \frac{1}{2(B^2 - D^2)} \left[ -(A^2 - 2MB + 2CD) \pm \sqrt{(A^2 - 2MB + 2CD)^2 - 4(B^2 - D^2)(M^2 - C^2)} \right] \quad (4)$$

which is obtained by solving  $E = C - Dk^2 + d(k) = 0$  for  $k$ . Here,  $\theta_{\pm}$  denote the incident angles for wavefunctions with wavenumber  $k_{\pm}$ . In the following, we set  $C = 0$  in the insulating side, when the Fermi energy is located at the middle of the gap. Notice that we assume insulating state so that  $k_{\pm}^2 < 0$ . Due to the translational symmetry along the  $y$ -axis, we have

$$k_F \sin \theta = k_+ \sin \theta_+ = k_- \sin \theta_-.$$

Boundary conditions read  $\psi(+0) = \psi(-0)$  and  $v_x \psi(+0) = v_x \psi(-0)$  with  $v_x = \frac{\partial H}{\partial k_x}$ . With these boundary conditions, we can obtain scattering coefficients.

Thus, the reflection coefficients for  $E_1$  state injection are obtained as follows

$$\begin{pmatrix} r_E \\ r'_E \end{pmatrix} = \frac{1}{\Delta_E} \begin{pmatrix} (Ak_+e^{i\theta_+} - a_+)(d(k_-) - M(k_-) + b_-) - (Ak_-e^{i\theta_-} - a_-)(d(k_+) - M(k_+) + b_+) \\ 2\{-b_+(d(k_-) - M(k_-)) + b_-(d(k_+) - M(k_+))\} \end{pmatrix} \quad (5)$$

with  $\Delta_E = (Ak_+e^{i\theta_+} + a_+)(d(k_-) - M(k_-) + b_-) - (Ak_-e^{i\theta_-} + a_-)(d(k_+) - M(k_+) + b_+)$ ,  $a_\sigma = (1 + \frac{B}{D})A\lambda_\sigma k_\sigma e^{i\theta_\sigma} - A(d(k_\sigma) - M(k_\sigma))/(2Dk_F \cos \theta)$ ,  $b_\sigma = -A^2 k_\sigma e^{i\theta_\sigma}/(2Dk_F \cos \theta) + (1 - \frac{B}{D})\lambda_\sigma(d(k_\sigma) - M(k_\sigma))$ ,  $\lambda_\sigma = k_\sigma \cos \theta_\sigma/(k_F \cos \theta)$ , and  $\sigma = \pm$ .

The corresponding reflection coefficients for spin down state can be obtained by the substitution  $A \rightarrow -A$  and  $\theta \rightarrow -\theta$ . Spin rotation angle  $\alpha$  is defined as  $\alpha = \text{Im} \log(r_{E\uparrow}/r_{E\downarrow})$ , which is the phase difference in the reflection coefficients between up and down spin electrons in the  $E$  state. From the definition, we see that  $\alpha$  is an odd function of  $\theta$  since  $r_{E\uparrow}(-\theta) = r_{E\downarrow}(\theta)$ . Note that when the spin of the incident electron is within the  $xy$ -plane, this angle  $\alpha$  gives the spin rotation angle within this plane at the reflection in the same band. Therefore, we call it "spin rotation angle".

Now, we show the results for  $\alpha$  in the plane of  $(\theta, M)$  in Fig. 2 for  $C = -0.08$  eV in (a),  $C = -0.1$  eV in (b), and  $C = -1$  eV in (c) with the other parameters fixed as  $A = 4$  eV  $\cdot \text{\AA}$ ,  $B = -70$  eV  $\cdot \text{\AA}^2$  and  $D = -50$  eV  $\cdot \text{\AA}^2$ . [17] In Figure 2 (a), a sharp ridge in  $M < 0$  and  $\theta > 0$  region and its negative correspondence in  $M < 0$  and  $\theta < 0$  are seen. This is in sharp contrast to the usual insulator case  $M > 0$  although  $\alpha$  is still nonzero there. Note that the height of the ridge is as high as  $\sim \pi/2$ . With increasing  $|C|$ , we find a qualitatively different structure. Near the origin in Fig. 2 (b),  $\alpha$  reaches  $\pi$ , changes its sign, and winds by  $4\pi$  around the origin, while it does not in the region far away from the origin. One might wonder that the singularity occurs at the origin and there is also an endpoint of the "branch cut" separating the  $4\pi$  winding and no winding. (Note that  $\alpha = \pi$  and  $\alpha = -\pi$  are equivalent and the continuous increase of  $\alpha$  in the clockwise direction is separated into several sheets). In fact, we have checked that  $\sin \alpha$ , which is physically observable, depends on the direction from which the origin is approached but it does not show any singularity at the endpoint of the "branch cut". As we further increase  $|C|$ , the branch cuts extend toward the larger  $|M|$  and  $|\theta|$  region, and approaches gradually to the negative  $M$ -axis as shown in Fig. 2 (c). Here, one may think that when magnetic field is applied in the  $xy$  plane and opens a gap, it will change our results when the Fermi level is inside the gap. However, magnitude of the gap is typically smaller than that of  $M$  ( $\sim 10$ meV), and the Fermi energy is shifted from the crossing of the helical edge dispersions. Hence, our results would be practically robust against applied magnetic field in realistic systems. Note

that all these interesting structures occur in the QSH region ( $M < 0$ ). It should be also noticed that these structures are seen for small  $\theta$ 's, i.e., almost normal incidence, and the relevance to the helical edge channel is expected. The angle at which the dispersions of the helical edge modes hit the Fermi energy is given by [18]

$$\theta_C = \pm \sin^{-1} \left[ \frac{MD}{Ak_F \sqrt{B^2 - D^2}} \right]. \quad (6)$$

We find that a large magnitude of  $\alpha$  in Fig. 2 appears around this angle, which means that the helical edge modes resonantly enhance the spin rotation. This is plausible since in the helical edge modes, up and down spins propagate in an opposite direction and hence SU(2) symmetry in spin space is strongly broken there. This is also similar to the Andreev reflection in the superconducting analogue of QSH system where the helical edge channel produces a largely spin-polarized supercurrent at the Andreev reflection. [19]

To realize the giant spin rotation experimentally, we propose QSH/N/QSH junction (see the inset in Fig. 3). When N layer is sufficiently thin, the electrons in the N region are in close contact to the QSH systems and the transport property in this junction is determined by the reflection at the interfaces. We will also take statistical and incident angular average of the results in order to obtain more experimentally accessible quantity.

To investigate spin rotation effect in this junction, we also have to calculate reflection coefficients with  $H$  state injection and  $E$  or  $H$  state reflection in a similar way. We consider the initial wavefunctions with density matrix as

$$\psi_i = \begin{pmatrix} a_1 \\ a_2 \\ a_3 \\ a_4 \end{pmatrix}, \quad \overline{a_i^* a_j} = \begin{cases} 1/4 & \text{for } \{i, j\} = \{1, 3\}, \{2, 4\} \\ 0 & \text{otherwise} \end{cases} \quad (7)$$

where  $\overline{\quad}$  denotes statistical average. The density matrix is chosen so that the initial wavefunctions have a correlation in the same bands. As seen in Eq. (7), here we consider the initial wavefunctions with spin polarization along  $x$ -axis. Using these expressions, we can obtain expectation values of  $\sigma_x$  and  $\sigma_y$ , Pauli matrices in spin space.

Figure 3 displays expectation values of  $\sigma_x$  and  $\sigma_y$  as a function of  $L/w$  for  $C = -1$  eV and  $M = -0.01$  eV. Here,  $L$  and  $w$  are the length and width of the N, respectively. An oscillatory dependence on  $L/w$  is seen because the phase difference between up and down spin

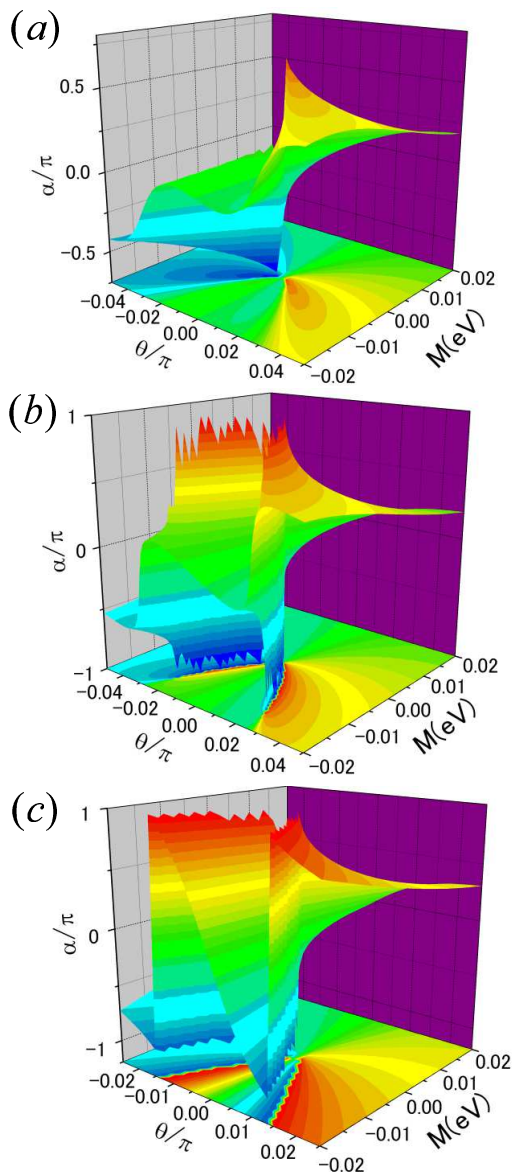


FIG. 2: (Color online) spin rotation angle  $\alpha$  as a function of injection angle and  $M$ . (a)  $C = -0.08$  eV, (b)  $C = -0.1$  eV and (c)  $C = -1$  eV. Note that  $\alpha = \pi$  and  $\alpha = -\pi$  are equivalent and the continuous increase of  $\alpha$  in the clockwise direction is separated into several sheets in (b) and (c).

states increases with  $L/w$ , namely the number of reflections. When  $\sigma_x$  has an extremum,  $\sigma_y$  almost vanishes and vice versa, which indicates a rotation of the spin in the  $xy$  plane in spin space upon propagation in the N of QSH/N/QSH junction. This means that the predicted giant spin rotation persists and is observable in realistic systems. Around  $L/w = 20$ , the initial spin is rotated by  $\pi$ . With  $w = 5\text{nm}$ , this giant spin rotation can be realized with the very short length scale of  $L = 100\text{nm}$ , which should be compared with that in the previous work[1] where the propagation of electron over  $1\mu\text{m}$  is required

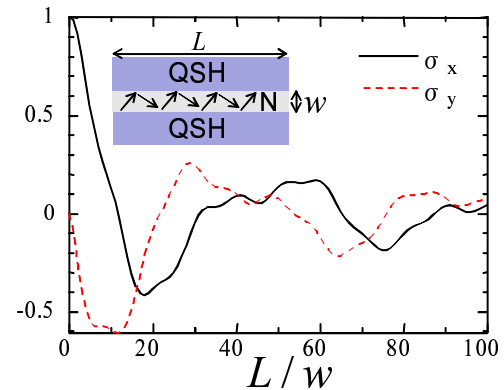


FIG. 3: (Color online) expectation values of  $\sigma_x$  and  $\sigma_y$  as a function of  $L/w$  for  $C = -1$  eV and  $M = -0.01$  eV. Inset shows the model.

to rotate electron spin by  $\pi$ . This may be a great advantage for application to nanotechnology.

In summary, we studied a reflection problem at the N/QSH interface and showed that an electron injected from the normal metal in N/QSH junctions shows a spin dependent reflection at the interface and hence there appears a phase difference between up and down spin states in the reflection coefficients. The spin rotation angle can be as large as  $\sim \pi$  in the QSH junction, because the helical edge modes resonantly enhance the spin rotation. In the QSH/N/QSH junction, multiple reflections at the interfaces increase the phase difference. This also results in a remarkable spin rotation effect in this junction even when the results are averaged over incident angles. The proposed Fabry-Pérot like heterostructure is experimentally accessible and could be used to unveil another aspect of the QSH state: *spin rotation effect*.

This work is supported by Grant-in-Aid for Scientific Research (Grant No. 17071007, 17071005) from the Ministry of Education, Culture, Sports, Science and Technology of Japan and NTT basic research laboratories. T.Y. acknowledges support by JSPS.

- 
- [1] S. Datta and B. Das, Appl. Phys. Lett. **56**, 665 (1990).
  - [2] J. Nitta, T. Akazaki, H. Takayanagi, and T. Enoki, Phys. Rev. Lett. **78**, 1335 (1997).
  - [3] M. I. D'yakonov and V. I. Perel', Phys. Lett. **35A**, 459 (1971); JETP Lett. **13**, 467 (1971).
  - [4] S. Murakami, N. Nagaosa, and S.-C. Zhang, Science **301**, 1348 (2003).
  - [5] Y. K. Kato, R. C. Myers, A. C. Gossard, and D. D. Awschalom, Science **306**, 1910 (2004).
  - [6] J. Wunderlich, B. Kaestner, J. Sinova, and T. Jungwirth, Phys. Rev. Lett. **94**, 047204 (2005).
  - [7] C. L. Kane and E. J. Mele, Phys. Rev. Lett. **95**, 146802 (2005); Phys. Rev. Lett. **95**, 226801 (2005).

- [8] B. A. Bernevig, and S. C. Zhang, Phys. Rev. Lett. **96**, 106802 (2006).
- [9] C. Wu, B. A. Bernevig, and S. C. Zhang, Phys. Rev. Lett. **96** 106401, (2006).
- [10] C. Xu and J. E. Moore, Phys. Rev. B **73** 045322, (2006).
- [11] L. Fu and C. L. Kane, Phys. Rev. B **74**, 195312 (2006); L. Fu and C. L. Kane, Phys. Rev. B **76**, 045302 (2007).
- [12] X.-L. Qi, T. Hughes, and S.-C. Zhang, arXiv:0802.3537v1.
- [13] B. A. Bernevig, T. L. Hughes, and S. C. Zhang, Science **314** 1757 (2006).
- [14] S. Murakami, S. Iso, Y. Avishai, M. Onoda, and N. Nagaosa, Phys. Rev. B **76**, 205304 (2007).
- [15] M. König, S. Wiedmann, C. Brüne, A. Roth, H. Buhmann, L. Molenkamp, X.-L. Qi, and S.-C. Zhang, Science, **318**, 766 (2007)
- [16] L. Molenkamp, private communications.
- [17] M. König, H. Buhmann, L. Molenkamp, T. Hughes, C-X Liu, X.-L. Qi, and S.-C. Zhang, J. Phys. Soc. Jpn. **77** 031007 (2008).
- [18] Bin Zhou, Hai-Zhou Lu, Rui-Lin Chu, Shun-Qing Shen and Qian Niu, Phys. Rev. Lett. **101**, 246807 (2008).
- [19] Y. Tanaka, T. Yokoyama, A. V. Balatsky, N. Nagaosa, arXiv:0806.4639v1.